Nonclassical oxygen atom transfer reactions of an eight-coordinate dioxomolybdenum(VI) complex

SCHOLARONE™
Manuscripts

Inorganic Chemistry Frontiers

ARTICLE

Nonclassical oxygen atom transfer reactions of an eight-coordinate dioxomolybdenum(VI) complex

Leila G. Ranis, Jacqueline Gianino, Justin M. Hoffman and Seth N. Brown*

The dioxomolybdenum(VI) complex $MoO_2Cl_2(dmf)_2$ reacts with $Pb(DOPO^Q)_2$ (DOPO = 2,4,6,8-tetra-*tert*-butyl-1,9-dioxophenoxazinate) to give $MoO_2(DOPO^Q)_2$, which has an eight-coordinate structure with normal molybdenum-oxo bond distances and angles but elongated distances to the dioxophenoxazine ligand. The dioxo complex is deoxygenated by phosphines to produce octahedral $Mo(DOPO^{Cat})_2$, in which reduction has taken place at the ancillary ligands. This compound in turn reacts with trimethylamine-*N*-oxide to regenerate $MoO_2(DOPO^Q)_2$, allowing a catalytic cycle for phosphine oxidation. This represents an example of four-electron nonclassical oxygen atom transfer in which both the oxidized and reduced forms of the metal complexes can be observed.

Introduction

Redox-active ligands are of interest for their ability to act as electron reservoirs in metal-mediated inner-sphere oxidation reactions.[1] Because such ligands can generally gain or lose up to two electrons, it becomes possible to gather four or more electrons worth of oxidizing or reducing equivalents around a single metal center, as for example in the formation of a bis(peroxo)zirconium(IV) complex from dioxygen and a zirconium(IV) bis(enediamide).[2]

One possible inner-sphere redox reaction is that of oxygen atom transfer (OAT).[3] We have described the reaction of oxomolybdenum bis(catecholate)[4] and molybdenum tris(catecholate)[5] complexes with pyridine-*N*-oxide to give, ultimately, $MoO_3(Opy)$. In these reactions, the metal forms new bonds to oxygen but remains in the +6 oxidation state, with all electrons for the reduction of pyridine-*N*-oxide to pyridine coming from the oxidation of the ligands from catecholate to *o*-benzoquinone. This division of labor results in a process that has been called a "nonclassical" oxygen atom transfer.[4] Unfortunately, these systems are not attractive candidates for catalytic oxygen atom transfer due to the instability of the oxidized species with respect to dissociation of *o*-benzoquinone. Indeed, even in cases where nonclassical catalytic nitrene transfer has been achieved, the active metal imido intermediate has not been isolated.[6,7,8]

An appealing strategy for stabilizing the oxidized forms of redox-active ligands against dissociation is to incorporate additional chelating groups in the ligand that maintain a negative charge even in their oxidized forms. Here we report the successful use of this strategy to enable the isolation of a dioxomolybdenum complex containing oxidized ligands and its

use in stoichiometric and catalytic oxygen atom transfer reactions.

Results and discussion

Preparation of dioxomolybdenum bis(2,4,6,8-tetra-*tert*-butyl-1,9-dioxophenoxazinate), $MoO_2(DOPO^Q)_2$

In the hopes of stabilizing the metal complex against dissociation of the ligand in its oxidized form, we turned to molybdenum and tungsten complexes of the ONO ligand (Chart 1). Despite its octahedral structure, $W(ONO^{Cat})_2$[9] rapidly deoxygenates two equivalents of *N*-methylmorpholine-*N*-oxide (NMO), forming one equivalent of $H(ONO^Q)$,[10] which is slowly oxidized to 2,4,6,8-tetra-*tert*-butylphenoxazin-1-one.[11] The metal-containing products are NMR-silent and could not be isolated or further characterized. $Mo(ONO^{Cat})_2$[12] reacted with NMO or Me_3NO analogously, but over the course of hours. Attempts to prepare an oxomolybdenum product by reacting $MoO_2Cl_2(dmf)_2$[13] with sources of $[ONO^Q]^-$ such as $Zn(ONO^Q)_2$[14] or $Pb(ONO^Q)_2$[15] also resulted in production of paramagnetic metal complexes as well as small amounts of the reduced complex $Mo(ONO^{Cat})_2$ and 2,4,6,8-tetra-*tert*-butylphenoxazin-1-one.

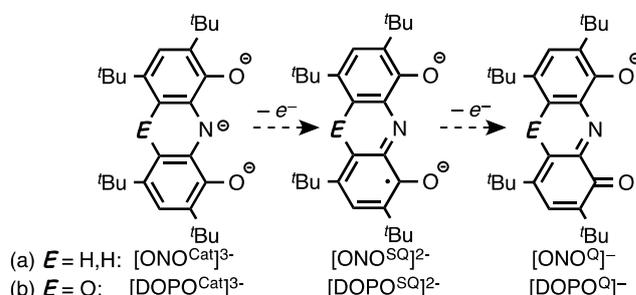Chart 1 Structures and oxidation states of the (a) ONO and (b) DOPO ligands.

(a) *E* = H,H: $[ONO^{Cat}]^{3-}$ $[ONO^{SQ}]^{2-}$ $[ONO^Q]^-$
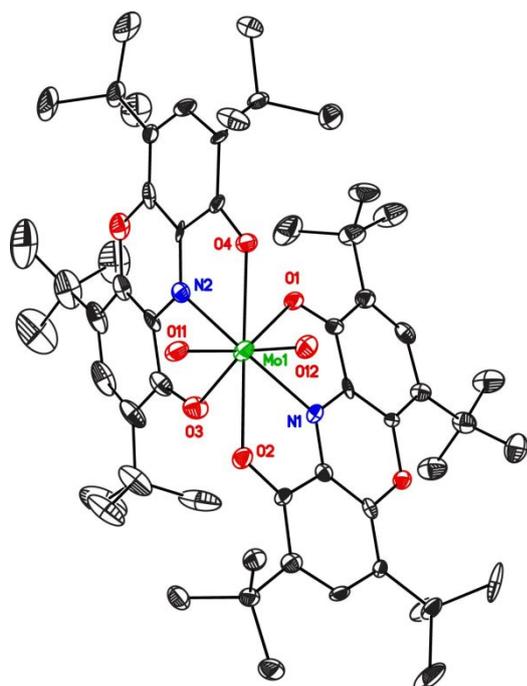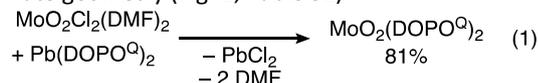(b) *E* = O: $[DOPO^{Cat}]^{3-}$ $[DOPO^{SQ}]^{2-}$ $[DOPO^Q]^-$

Attempts to prepare an oxidized complex with the more robust oxygen-bridged DOPO (2,4,6,8-tetra-*tert*-butyl-1,9-

Department of Chemistry and Biochemistry, University of Notre Dame,
251 Nieuwland Science Hall, Notre Dame, IN 46556-5670, USA.
Email: Seth.N.Brown.114@nd.edu

dioxophenoxazinate, Chart 1) ligand[16] proved more fruitful. Reaction of Pb(DOPO^Q)$_2$[12] with MoO$_2$Cl$_2$(dmf)$_2$ in chlorinated solvents gives good yields of deep blue, highly moisture-sensitive MoO$_2$(DOPO^Q)$_2$ (eq 1). ^{1}H and ^{13}C NMR spectra of this diamagnetic material show, unusually, two different arene environments of equal intensity for the DOPO ligands, suggesting a nonfluxional C_2-symmetric structure. This is borne out by the solid-state structure, which shows an eight-coordinate geometry (Fig. 1, Table S1).

$$\begin{array}{c} \text{MoO}_2\text{Cl}_2\text{(DMF)}_2 \\ + \text{Pb(DOPO}^Q)_2 \end{array} \xrightarrow[\substack{-\text{PbCl}_2 \\ -2\text{ DMF}}]{} \begin{array}{c} \text{MoO}_2\text{(DOPO}^Q)_2 \\ 81\% \end{array} \quad (1)$$

Fig. 1 Thermal ellipsoid plot (50% thermal ellipsoids) of one of the crystallographically inequivalent molecules of MoO$_2$(DOPO^Q)$_2$. Hydrogen atoms are omitted for clarity. Selected distances and angles, averaged over the chemically equivalent values in the crystal: Mo–O11, 1.688(4) Å; Mo–O1, 2.26(2) Å; Mo–N1, 2.350(13) Å; Mo–O2, 2.312(16) Å; O11–Mo–O12, 105.0(7)°.

Previously characterized dioxomolybdenum(VI) complexes are almost all six- or lower-coordinate, as expected due to the *cis*-dioxo fragment's ability to form three π bonds and thus donate ten electrons. One nominally seven-coordinate complex, [(tacn)MoO$_2$(η^2-MeNHO)]ClO$_4$ (tacn = 1,4,7-triazacyclononane), containing an η^2-hydroxylamine ligand, has been prepared.[17] Only one example of an eight-coordinate dioxomolybdenum(VI) complex has been observed previously.[18] This complex, which contains two tridentate 2,4-di-*tert*-butyl-6-(pyridin-2-ylazo)phenolate ligands and has a geometry very similar to that of MoO$_2$(DOPO^Q)$_2$, was assigned as a distorted square antiprism despite the fact that the two trapezoids formed by the ligating atoms of the chelate plus an oxo group lie in nearly perpendicular planes (θ = 89.1°; compare θ = 87.9°, 88.2° for the two crystallographically inequivalent molecules of MoO$_2$(DOPO^Q)$_2$). As noted by Lippard and Russ,[19] this feature in eight-coordinate complexes

is diagnostic of dodecahedral geometry (θ_{ideal} = 90°, compared to θ_{ideal} = 77.4° for a square antiprism). The eight-coordinate geometry is thus better described as dodecahedral. A uranium complex UO$_2$(DOPO^Q)$_2$ shares a similar formula with MoO$_2$(DOPO^Q)$_2$ and is also eight-coordinate, but is structurally quite different, with a *trans*-dioxo (uranyl) moiety and a hexagonal bipyramidal geometry.[20]

Remarkably, the dioxomolybdenum moiety in MoO$_2$(DOPO^Q)$_2$ is essentially unperturbed structurally (d_{MoO} = 1.688(4) Å avg, OMoO = 105.0(7)° avg)[21] and spectroscopically (ν_{MoO2} = 911, 951 cm^{-1})[22] from typical octahedral dioxomolybdenum complexes. Instead, the supersaturation of the molybdenum center is reflected in the extremely long bonds to the DOPO ligand, which show 0.26–0.31 Å longer Mo–O bonds and 0.38 Å longer Mo–N bonds than in Mo(DOPO^{Cat})$_2$.[12] Some of this elongation is due to the oxidation of the ligand to the quinonoid oxidation state, but a similar ligand oxidation from (ONO^{Cat})ZrCl(THF)$_2$ to (ONO^Q)$_2$Zr$_2$Cl$_4$(μ-OH)$_2$ induces elongations of only 0.12 Å in the Zr–O and 0.21 Å in the Zr–N bonds,[23] suggesting a ~0.17 Å elongation induced by the high coordination number of the dioxomolybdenum(VI) fragment. Eight-coordination is retained in solution, as judged by NMR. Specifically, partial dissociation of a ligand to form a six-coordinate structure containing a κ^1-DOPO ligand would generate a molecular mirror plane, and thus does not appear to be facile, given the nonfluxional, C_2-symmetric NMR spectra (Fig. S1).

While the DOPO ligand is redox-active, there can be no doubt that it adopts the quininonoid, monoanionic oxidation state in MoO$_2$(DOPO^Q)$_2$, as any more reduced state would require molybdenum to adopt a physically impossible oxidation state greater than +6. This oxidation state is consistent with the intraligand distances observed crystallographically, for which established correlations[12] give an average "metrical oxidation state" (MOS)[24] of −1.30(18), equal to −1 within experimental error. Density functional theory (DFT) calculations confirm this oxidation state assignment, giving equivalent structural data (DFT MOS = −1.17(19) avg.) and showing that the DOPO redox-active orbitals (the HOMO of the catecholate form or the LUMO of the quinone form[25]) appear as the LUMO and LUMO+1 of the complex, and are almost completely ligand-centered (Fig. 2).

Stoichiometric and catalytic oxygen atom transfer reactions of MoO$_2$(DOPO^Q)$_2$

Mo(DOPO^{Cat})$_2$ and MoO$_2$(DOPO^Q)$_2$ comprise a four-electron, two oxygen atom redox couple. Interconversions between the species have been realized with appropriate oxygen atom donors and acceptors (Scheme 1). In particular, phosphines such as PPh$_3$ and PMe$_2$Ph quantitatively deoxygenate MoO$_2$(DOPO^Q)$_2$ over the course of 24 h and 20 min, respectively, to form two equivalents of OPR$_3$ and Mo(DOPO^{Cat})$_2$. Triphenylarsine reacts similarly, but much more slowly (6 d at RT). Other substrates such as norbornene, diphenylacetylene, and tetrahydrothiophene are not oxidized by Mo(DOPO^{Cat})$_2$ even over days at 70 °C. In the oxidative direction, Me$_3$NO reacts immediately with Mo(DOPO^{Cat})$_2$ to

2 | *Inorg. Chem. Front.*, 2021, **8**, 1-6

This journal is © The Partner Organisations 2021
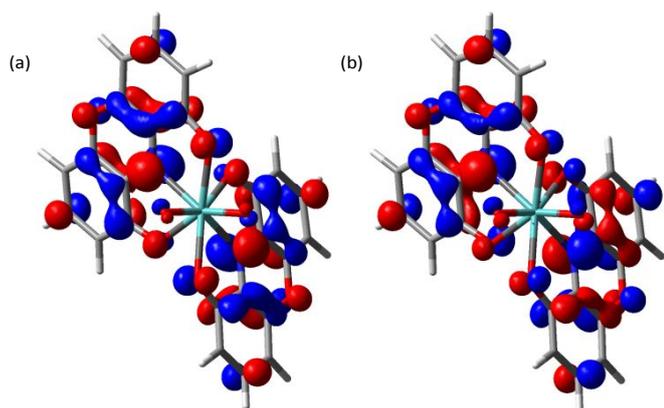
Fig. 2 Kohn-Sham orbitals of $MoO_2(DOPO^Q)_2$ (B3LYP, 6-31G*/SDD for Mo). (a) LUMO (*A* symmetry). (b) LUMO+1 (*B* symmetry).

give $MoO_2(DOPO^Q)_2$ in ~70% yield (by ^{1}H NMR integration against an internal standard). $W(DOPO^{Cat})_2$ reacts analogously to give $WO_2(DOPO^Q)_2$, as judged by NMR, though this compound has not been isolated. *N*-Methylmorpholine-*N*-oxide also reacts rapidly with $Mo(DOPO^{Cat})_2$, but generates mostly $HDOPO^Q$ and paramagnetic Mo-containing materials, with only about 5% of $MoO_2(DOPO^Q)_2$ being formed. Dioxygen reacts slowly (1 d at 70 °C) with $Mo(DOPO^{Cat})_2$, but only traces of $MoO_2(DOPO^Q)_2$ are formed. Pyridine-*N*-oxide is not deoxygenated even at elevated temperatures. Presumably the oxygen atom transfer reactions proceed through the intermediacy of a monooxo complex, but this has not been observed in either oxidation or reduction reactions.
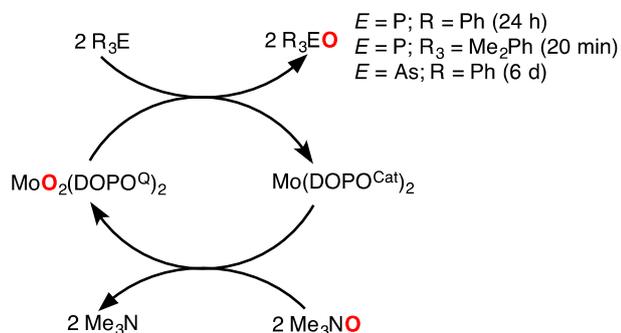
Scheme 1. Oxygen atom transfer reactions of the $Mo(DOPO^{Cat})_2/MoO_2(DOPO^Q)_2$ couple.

The accessibility of both oxidative and reductive OAT reactions opens the possibility of catalysis, which has been realized in oxidations of phosphines with trimethylamine-*N*-oxide, although the low yield of reoxidation to $MoO_2(DOPO^Q)_2$ limits the number of turnovers. For example, only 1.5 turnovers are achieved in 24 h in the $Mo(DOPO^{Cat})_2$-catalyzed oxidation of PPh_3 by Me_3NO. Dimethylphenylphosphine is oxidized more efficiently, with 20 turnovers achieved in 2 h at 23 °C.

The electronic structure of $Mo(DOPO^{Cat})_2$ appears to be well described as a Mo(VI) complex of a fully reduced $DOPO^{3-}$ ligand (MOS = −2.83(23)).[12] Since the oxidation states of the ligands, but not the metal, change when $Mo(DOPO^{Cat})_2$ and $MoO_2(DOPO^Q)_2$ interconvert, these are examples of nonclassical oxygen atom transfer. There are a number of

unusual features of this redox couple. First, this is an example where both the oxidized and reduced forms of such a couple can be observed. In many cases, the oxidized form of the ligand dissociates rapidly (for example, as a neutral *o*-benzoquinone[4,5] or 2,2'-bipyridine[26]), rendering the oxidized complex unobservable. In other cases, the oxidized form of the complex is so reactive that it can only be inferred as a transient species.[27] The $Mo(DOPO^{Cat})_2/MoO_2(DOPO^Q)_2$ pair is also unusual in being a *four*-electron redox couple. Examples of dioxometal complexes that undergo classical four-electron oxygen atom transfer reactions are known,[28] but this appears to be the first example where ligand-centered redox changes provide the impetus for such a reaction.

A limitation of the present system is its relatively low reactivity. A possible reason for this is that is the poor coupling between the ligand-centered redox system and the π* orbitals of the dioxomolybdenum unit, which are well separated in energy (calculated to be 1.45 eV apart) and interact only minimally (Fig. 2). Explorations of later transition metal complexes, where the metal *d* orbitals are closer in energy to the redox-active ligand frontier orbitals, are underway to see if these electronic changes can induce greater coupling between the oxometal and ligand orbitals and foster enhanced reactivity.[29,30]

Conclusions

Despite its apparent coordinative saturation, six-coordinate $Mo(DOPO^{Cat})_2$ readily deoxygenates trimethylamine-*N*-oxide to form eight-coordinate $MoO_2(DOPO^Q)_2$. The eight-coordinate geometry is dodecahedral, containing a typical dioxomolybdenum(VI) fragment ligated by two κ³-DOPO ligands with highly elongated Mo–O and Mo–N bonds. Since $Mo(DOPO^{Cat})_2$ has been characterized as containing Mo(VI) and fully reduced, trianionic DOPO ligands, and since $MoO_2(DOPO^Q)_2$ must contain Mo(VI) and fully oxidized, monoanionic DOPO ligands, this reaction constitutes a double oxygen atom transfer reaction where all four electrons come from the ligand rather than the metal (a nonclassical redox reaction). Phosphines and arsines can deoxygenate $MoO_2(DOPO^Q)_2$, allowing oxygen atom transfer catalysis between phosphines and Me_3NO, though turnover numbers are limited by catalyst decomposition during oxidation.

Experimental Section

General procedures

All procedures were carried out under an inert atmosphere in a nitrogen-filled glovebox or on a vacuum line. Chlorinated solvents and acetonitrile were dried over 4 Å molecular sieves, followed by CaH_2. $MoO_2Cl_2(dmf)_2$[13] and $Pb(DOPO^Q)_2$[12] were prepared by literature methods. NMR spectra were measured on a Bruker Avance DPX 400 MHz or 500 MHz spectrometer. Chemical shifts for ^{1}H and [13]C{[1]H} spectra are reported in ppm downfield of TMS, with spectra referenced using the known chemical shifts of the solvent residuals. Infrared spectra were

This journal is © The Partner Organisations 2021

Inorg. Chem. Front., 2021, **8**, 1-6 | **3**

ARTICLE   **Inorganic Chemistry Frontiers**

recorded as nujol mulls on a JASCO FT/IR-6300 spectrometer. Elemental analyses were performed by Midwest Microanalytical Laboratories (Indianapolis, IN).

Synthesis of dioxobis(2,4,6,8-tetra-*tert*-butyl-9-oxyphenoxazin-1-onato)molybdenum(VI), MoO₂(DOPO^Q)₂

In the drybox, 131.4 mg of $MoO_2Cl_2(dmf)_2$ (0.381 mmol) and 324.4 mg of $Pb(DOPO^Q)_2$ (0.79 equiv) were weighed into a 20 mL scintillation vial and dissolved in 5 mL chloroform. The vial was capped and the solution stirred 24 h. The reaction mixture was filtered through a fine porosity glass frit to remove $PbCl_2$. The solvent was evaporated on the vacuum line, leaving an oily dark blue residue that hardened into a glass. The product was triturated with acetonitrile, then filtered through a fine porosity glass frit. The crude product was dissolved in 2 mL dichloromethane and layered with 8 mL acetonitrile. After 3 d at −20 °C, the crystals were filtered and washed with minimal acetonitrile to recover 244.5 mg (81%) $MoO_2(DOPO^Q)_2$. ¹H NMR (CD_2Cl_2): δ 0.91, 1.40, 1.41, 1.49 (s, 18H each, ^tBu), 7.39, 7.62 (s, 2H each, Ar*H*). ¹³C{¹H} NMR (CD_2Cl_2): δ 29.0, 29.5, 30.26, 30.31 (C(*C*H₃)₃); 34.5, 34.8, 34.9, 35.4 (*C*(CH₃)₃); 123.2, 124.6, 132.6, 135.1, 135.9, 137.4, 137.6, 137.7, 142.5, 143.2 (aromatics); 172.6, 173.0 (*C*OMo). IR (cm⁻¹): 3158 (w), 1587 (s), 1540 (m), 1366 (s), 1289 (w), 1230 (s), 1165 (m), 1074 (m), 1042 (m), 1021 (m), 1012 (m), 974 (w), 951 (w, ν_MoO), 928 (w), 911 (w, ν_MoO), 878 (w), 814 (w), 770 (w), 697 (w). Anal. Calcd. for $C_{56}H_{76}MoN_2O_8$: C, 67.18; H, 7.65; N, 2.80. Found: C, 65.35; H, 7.48; N, 2.87.

Catalytic oxidation of phosphines by trimethylamine-*N*-oxide

Catalytic studies were carried out in CD_2Cl_2 at ambient temperature (23 °C) using Mo(DOPO)₂ as precatalyst. Reactions were monitored by ¹H NMR and reaction progress was measured by integration of the signals due to unreacted phosphine and to phosphine oxide; no other phosphine-derived signals were apparent by NMR. Trimethylamine was observed as the sole reduction product of the *N*-oxide, but was not used in quantitation because of its possible partitioning into the gas phase. In a typical reaction, Mo(DOPO^Cat)₂ (4.1 mg, 4.2 μmol), Me₃NO (21.2 mg, 282 μmol, 67 equiv), and PMe₂Ph (20.0 μL, 141 μmol, 33 equiv) were loaded into a sealable NMR tube in the glovebox. Dichloromethane-d_2 (0.7 mL) was added and the tube was sealed and taken out of the glovebox to be monitored by ¹H NMR spectroscopy. Control experiments establish that neither PPh₃ nor PMe₂Ph reacts appreciably with Me₃NO in CD_2Cl_2 at 23 °C over the timespan of the reaction (2 h for PMe₂Ph, 24 h for PPh₃) in the absence of a catalyst.

X-ray crystallography

Vapor diffusion of acetonitrile into a dichloromethane solution of MoO₂(DOPO)₂ in the drybox yielded small crystals. One 0.11 × 0.09 × 0.07 specimen was placed in Paratone oil before being transferred to the cold N₂ stream of a Bruker Apex II CCD diffractometer in a nylon loop. The crystal diffracted weakly; reflections were observable only to 0.8 Å resolution, and upon data processing and refinement, reflections below 1.0 Å

resolution were omitted. Data were reduced, correcting for absorption, using the program SADABS. The structure was solved using direct methods. All nonhydrogen atoms were refined anisotropically. One atom, C45, could not be refined anisotropically in an unconstrained refinement, so its thermal parameters were restrained to be approximately isotropic with an esd of 0.002 using the ISOR command in SHELXL. All hydrogen atoms were placed in calculated positions. Calculations used SHELXTL (Bruker AXS),[31] with scattering factors and anomalous dispersion terms taken from the literature.[32] Further details about the structure are given in Table S1 and selected distances and angles are listed in Tables S2-S3.

Computational Methods

Geometry optimizations were performed on (DOPO)₂MoO₂ in the singlet state using density functional theory (B3LYP, SDD basis set for Mo, 6-31G* for other atoms) as implemented in the Gaussian16 suite of programs.[33] The X-ray structure, rendered strictly C_2-symmetric, was used as an initial geometry, with *tert*-butyl groups replaced by hydrogen. The optimized geometry was confirmed as a minimum by calculation of vibrational frequencies. Plots of calculated Kohn–Sham orbitals were generated using Gaussview (v. 6.0.16) with an isovalue of 0.04.

Conflicts of interest

There are no conflicts to declare.

Acknowledgements

Notes and references

1   (a) V. Lyaskovskyy and B. de Bruin, Redox Non-Innocent Ligands: Versatile New Tools to Control Catalytic Reactions, *ACS Catal.*, 2012, **2**, 270-279. (b) R. F. Munhá, R. A. Zarkesh and A. F. Heyduk, Group transfer reactions of d⁰ transition metal complexes: redox-active ligands provide a mechanism for expanded reactivity, *Dalton Trans.*, 2013, **42**, 3751-3766. (c) D. L. J. Broere, R. Plessius and J. I. van der Vlugt, New avenues for ligand-mediated processes – expanding metal reactivity by the use of redox-active catechol, *o*-aminophenol and *o*-phenylenediamine ligands, *Chem. Soc. Rev.*, 2015, **44**, 6886-6915.

2   C. Stanciu, M. E. Jones, P. E. Fanwick and M. M. Abu-Omar, Multi-electron Activation of Dioxygen on Zirconium(IV) to Give an Unprecedented Bisperoxo Complex, *J. Am. Chem. Soc.*, 2007, **129**, 12400-12401.

3   R. H. Holm and J. P. Donahue, A thermodynamic scale for

oxygen atom transfer reactions, *Polyhedron*, 1993, **12**, 571-589.

4　T. Marshall-Roth, S. C. Liebscher, K. Rickert, N. J. Seewald, A. G. Oliver and S. N. Brown, Nonclassical oxygen atom transfer reactions of oxomolybdenum(VI) bis(catecholate), *Chem. Commun.*, 2012, **48**, 7826-7828.

5　A. H. Randolph, N. J. Seewald, K. Rickert and S. N. Brown, Tris(3,5-di-*tert*-butylcatecholato)molybdenum(VI): Lewis Acidity and Nonclassical Oxygen Atom Transfer Reactions, *Inorg. Chem.*, 2013, **52**, 12587-12598.

6　A. I. Nguyen, R. A. Zarkesh, D. C. Lacy, M. K. Thorson and A. F. Heyduk, Catalytic nitrene transfer by a zirconium(IV) redox-active ligand complex, *Chem. Sci.*, 2011, **2**, 166-169.

7　A. F. Heyduk, R. A. Zarkesh and A. I. Nguyen, Designing Catalysts for Nitrene Transfer Using Early Transition Metals and Redox-Active Ligands, *Inorg. Chem.*, 2011, **50**, 9849-9863.

8　(a) N. P. van Leest, M. A. Tepaske, J.-P. H. Oudsen, B. Venderbosch, N. R. Rietdijk, M. A. Siegler, M. Tromp, J. I. van der Vlugt and B. de Bruin, Ligand Redox Noninnocence in [Co^{III}(TAML)]$^{0/-}$ Complexes Affects Nitrene Formation, *J. Am. Chem. Soc.*, 2020, **142**, 552-563. (b) N. P. van Leest, M. A. Tepaske, B. Venderbosch, J.-P. H. Oudsen, M. Tromp, J. I. van der Vlugt and B. de Bruin, Electronically Asynchronous Transition States for C–N Bond Formation by Electrophilic [Co^{III}(TAML)]-Nitrene Radical Complexes Involving Substrate-to-Ligand Single-Electron Transfer and a Cobalt-Centered Spin Shuttle, *ACS Catal.*, 2020, **10**, 7449-7463.

9　D. W. Shaffer, G. Szigethy, J. W. Ziller and A. F. Heyduk, Synthesis and Characterization of a Redox-Active Bis(thiophenolato)amide Ligand, [SNS]$^{3-}$, and the Homoleptic Tungsten Complexes, W[SNS]$_2$ and W[ONO]$_2$, *Inorg. Chem.* 2013, **52**, 2110-2118.

10　A. I. Poddel'sky, N. N. Vavilina, N. V. Somov, V. K. Cherkasov and G. A. Abakumov, Triethylantimony(V) complexes with bidentate *O,N-, O,O-* and tridentate *O,N,O'*-coordinating *o*-iminoquinonato/*o*-quinonato ligands: Synthesis, structure and some properties, *J. Organomet. Chem.*, 2009, **694**, 3462-3469.

11　(a) H. B. Stegmann and K. Scheffler, ESR-Untersuchungen einer Modell-Phenoxazinsynthese, *Chem. Ber.*, 1968, **101**, 262-271. (b) G. Fukata, N. Sakamoto and M. Tashiro, Cyclodienones. Part 6. Preparation of 4-Azido-2,4,6-tri-t-butylcyclohexa-2,5-dienone and its Thermal, Photo-, and Acid-catalyzed Decomposition, *J. Chem. Soc. Perkin Trans. 1*, 1982, 2841-2848. (c) R. F. X. Klein, L. M. Bargas and V. Horak, Oxidative Deamination of *sec*-Alkyl Primary Amines with 3,5-Di-*tert*-butyl-1,2-benzoquinone: A Second Look, *J. Org. Chem.* 1988, **53**, 5994-5998. (d) S. Bhattacharya and C. G. Pierpont, Semiquinone Imine Complexes of Ruthenium. Coordination and Oxidation of the 1-Hydroxy-2,4,6,8-tetra-*tert*-butylphenoxazinyl Radical, *Inorg. Chem.* 1992, **31**, 2020-2029.

12　L. G. Ranis, K. Werellapatha, N. J. Pietrini, B. A. Bunker and S. N. Brown, Metal and Ligand Effects on Bonding in Group 6 Complexes of Redox-Active Amidodiphenoxides, *Inorg. Chem.*, 2014, **53**, 10203-10216.

13　F. J. Arnaiz, R. Aguado, J. Sanz-Aparicio and M. Martinez-Ripoll, Addition Compounds of Dichlorodioxomolybdenum(VI) from Hydrochloric Acid Solutions of Molybdenum Trioxide. Crystal Structure of Dichlorodioxodiaquamolybdenum(VI) bis(2,5,8-trioxanonane), *Polyhedron* 1994, **13**, 2745-2749.

14　A. Y. Girgis and A. L. Balch, Catechol Oxidations. Characterization of Metal Complexes of 3,5,-Di-*tert*-butyl-1,2-quinone 1-(2-Hydroxy-3,5-di-*tert*-butylphenyl)imine Formed by the Aerial Oxidation of 3,5-Di-*tert*-butylcatechol in the Presence of Ammonia and Divalent Metal Ions, *Inorg. Chem.* 1975, **14**, 2724-2727.

15　(a) B. R. McGarvey, A. Ozarowski, Z. Tian and D. G. Tuck, Tin and lead derivatives of a Schiff base – bis(orthoquinone) ligand, *Can. J. Chem.* 1995, **73**, 1213-1222. (b) S. Shekar and S. N. Brown, Migrations of Alkyl and Aryl Groups from Silicon to Nitrogen in Silylated Aryloxyiminoquinones, *Organometallics* 2013, **32**, 556-564.

16　(a) V. I. Simakov, Y. Y. Gorbanev, T. E. Ivakhnenko, V. G. Zaletov, K. A. Lyssenko, Z. A. Starikova, E. P. Ivakhnenko and V. I. Minkin, Synthesis, chemical properties, and crystal structure of 2,4,6,8-tetra(*tert*-butyl)-9-hydroxyphenoxazin-1-one, *Russ. Chem. Bull.* 2009, **58**, 1361-1370. (b) E. P. Ivakhnenko, A. G. Starikov, V. I. Minkin, K. A. Lyssenko, M. Y. Antipin, V. I. Simakov, M. S. Korobov, G. S. Borodkin and P. A. Knyazev, Synthesis, Molecular and Electronic Structures of Six-Coordinate Transition Metal (Mn, Fe, Co, Ni, Cu, and Zn) Complexes with Redox-Active 9-Hydroxyphenoxazin-1-one Ligands, *Inorg. Chem.*, 2011, **50**, 7022-7032.

17　C. Hauser, T. Weyhermüller and K. Wieghardt, Reductive nitrosylation of V$_2$O$_5$ and MoO$_3$ with hydroxylamine in the presence of 1,4,7-triazacyclononane, *Coll. Czech. Chem. Commun.*, 2001, **66**, 125-138.

18　I. Chatterjee, N. S. Chowdhury, P. Ghosh and S. Goswami, Octacoordinated Dioxo-Molybdenum Complex via Formal Oxidative Addition of Molecular Oxygen. Studies of Chemical Reactions Between M(CO)$_6$ (M = Cr, Mo) and 2,4-Di-*tert*-butyl-6-(pyridin-2-ylazo)-phenol, *Inorg. Chem.*, 2015, **54**, 5257-5265.

19　S. J. Lippard and B. J. Russ, Comment on th Choice of an Eight-Coordinate Polyhedron, *Inorg. Chem.*, 1968, **7**, 1686-1688.

20　S. A. Pattenaude, C. S. Kuehner, W. L. Dorfner, E. J. Schelter, P. E. Fanwick and S. C. Bart, Spectroscopic and Structural Elucidation of Uranium Dioxophenoxazine Complexes, *Inorg. Chem.*, 2015, **54**, 6520-6527.

21　J. M. Mayer, Metal–Oxygen Multiple Bond Lengths: A Statistical Study, *Inorg. Chem.*, 1988, **27**, 3899-3903.

22　J. Topich and J. O. Bachert, Solution IR Spectroscopic Studies of *cis*-Dioxomolybdenum(VI) Complexes, *Inorg. Chem.*, 1992, **31**, 511-515.

23　F. Lu, R. A. Zarkesh and A. F. Heyduk, A Redox-Active Ligand as a Reservoir for Protons and Electrons: O$_2$ Reduction at Zirconium(IV), *Eur. J. Inorg. Chem.*, 2012, 467-470.

24　S. N. Brown, Metrical Oxidation States of 2-Amidophenoxide and Catecholate Ligands: Structural Signatures of Metal–Ligand π Bonding in Potentially Noninnocent Ligands, *Inorg. Chem.*, 2012, **51**, 1251-1260.

25　T. Ren, Transition metal complexes of a tridentate biquinone ligand: electronic structures, charge distributions and magnetic properties, *Inorg. Chim. Acta*, 1995, **229**, 195-202.

26　(a) G. Zi, L. Jia, E. L. Werkema, M. D. Walter, J. P. Gottfriedsen and R. A. Andersen, Preparation and Reactions of Base-Free Bis(1,2,4-tri-*tert*-butylcyclopentadienyl)uranium Oxide, Cp'$_2$UO, *Organometallics* **2005**, *24*, 4251-4264. (b) W. Ren, G. Zi and M. D. Walter, Synthesis, Structure, and Reactivity of a Thorium Metallocene Containing a 2,2'-Bipyridyl Ligand, *Organometallics* **2012**, *31*, 672-679.

27　D. D. Wright and S. N. Brown, Nonclassical Oxygen Atom Transfer as a Synthetic Strategy: Preparation of an Oxorhenium(V) Complex of the Bis(3,5-di-*tert*-butyl-2-

phenoxo)amide Ligand, *Inorg. Chem.* **2013**, *52*, 7381-7383.

28 (a) A. Dovletoglou and T. J. Meyer, Mechanism of *cis*-Directed Four-Electron Oxidation by a *trans*-Dioxo Complex of Ruthenium(VI), *J. Am. Chem. Soc.*, 1994, **116**, 215-223. (b) M. R. Lentz, J. S. Vilardo, M. A. Lockwood, P. E. Fanwick and I. P. Rothwell, Reduction of Dioxygen, N=N, and N=O Double Bonds by Tungsten(II) Aryloxide Compounds, *Organometallics*, 2004, **23**, 329-343. (c) N. Tsvetkov, M. Pink, H. Fan, J.-H. Lee and K. G. Caulton, Redox and Lewis Acid Reactivity of Unsaturated Os^{II}, *Eur. J. Inorg. Chem.*, 2010, 4790-4800.

29 J. M. Hoffman, A. G. Oliver and S. N. Brown, The Metal or the Ligand? The Preferred Locus for Redox Changes in Oxygen Atom Transfer Reactions of Rhenium Amidodiphenoxides, *J. Am. Chem. Soc.*, 2017, **139**, 4521-4531.

30 A. N. Erickson, J. Gianino, S. J. Markovitz and S. N. Brown, Amphiphilicity in Oxygen Atom Transfer Reactions of Oxobis(iminoxolene)osmium Complexes, *Inorg. Chem.*, 2021, **60**, ASAP (DOI: 10.1021/acs.inorgchem.1c00068).

31 G. M. Sheldrick, A short history of *SHELX*, *Acta Crystallogr., Sect. A: Found. Crystallogr.*, 2007, **64**, 112-122.

32 A. J. C. Wilson, *International Tables for Crystallography*, Kluwer Academic Publishers, Dordrecht, The Netherlands, 1992, vol. C.

33 M. J. Frisch, G. W. Trucks, H. B. Schlegel, G. E. Scuseria, M. A. Robb, J. R. Cheeseman, G. Scalmani, V. Barone, G. A. Petersson, H. Nakatsuji, X. Li, M. Caricato, A. V. Marenich, J. Bloino, B. G. Janesko, R. Gomperts, B. Mennucci, H. P. Hratchian, J. V. Ortiz, A. F. Izmaylov, J. L. Sonnenberg, D. Williams-Young, F. Ding, F. Lipparini, F. Egidi, J. Goings, B. Peng, A. Petrone, T. Henderson, D. Ranasinghe, V. G. Zakrzewski, J. Gao, N. Rega, G. Zheng, W. Liang, M. Hada, M. Ehara, K. Toyota, R. Fukuda, J. Hasegawa, M. Ishida, T. Nakajima, Y. Honda, O. Kitao, H. Nakai, T. Vreven, K. Throssell, J. A. Montgomery Jr., J. E. Peralta, F. Ogliaro, M. J. Bearpark, J. J. Heyd, E. N. Brothers, K. N. Kudin, V. N. Staroverov, T. A. Keith, R. Kobayashi, J. Normand, K. Raghavachari, A. P. Rendell, J. C. Burant, S. S. Iyengar, J. Tomasi, M. Cossi, J. M. Millam, M. Klene, C. Adamo, R. Cammi, J. W. Ochterski, R. L. Martin, K. Morokuma, O. Farkas, J. B. Foresman and D. J. Fox, *Gaussian 16, Revision B.01*, Gaussian, Inc., Wallingford CT, 2016.